Building Blocks for Molecule-Based Magnets: A Theoretical Study of Triplet−Singlet Gaps in the Dianion of Rhodizonic Acid 1,4-Dimethide and Its Derivatives

Andrzej W. Misiołek*,† and James E. Jackson*

Contribution from the Department of Chemistry, Michigan State University, East Lansing, Michigan 48824

Received June 14, 2000

Abstract: Reduction of 1,4-dimethylenecyclohexane-2,3,5,6-tetrone forms the title dianion $\mathbf{1}^{2-}$, which may also be formulated as the 1,4-dimethide of deprotonated rhodizonic acid. Substituted versions of this species, designed as a charged electronic analogue of dimethylenecyclobutadiene, are proposed as building blocks for assembly of molecule-based magnets. A possible mode of self-organization of their metal salts into 2-D structures with intermolecular ferromagnetic coupling is outlined. Full π space CAS(14,12)/6-31+G*//CAS(14,12)/6-31G* calculations were performed to probe the ground spin state (singlet vs triplet) of $\mathbf{1}^{2-}$ as a function of substituent variations. This study has found that a triplet ground state preference as high as 4.5 kcal/mol may be achieved for the symmetrically coordinated dianion.

Introduction

Conjugated diradicals have fascinated theoretical chemists since the discovery of the “Schlenk hydrocarbon” in 1915.[1] Recently additional interest in this class of species[2] has centered on their potential as paramagnetic building blocks for formation of molecule-based organic magnetic materials.[3] This use requires self-assembly into magnetically coupled networks with extended, multidimensional topologies. One possible assembly strategy is to organize organic radical and polyradical ligands via complexation to metal cations.[4] In such solids the bridging cations may also function as electron spin relays and/or carriers. Most stable radicals and polyradicals known to date, however, have undesirable (weak or poorly defined) coordination and coupling abilities, having typically been selected for their lack of reactivity. As a means to enforce strong interactions through bridging metal cations, a number of research groups have explored the incorporation of multiple coordination sites and anionic groups into organic radical building blocks. Despite some success[4,5] for the most part those efforts have been frustrating, including our own attempts.[6] The main problem has been that strong extended communication in more than one dimension in a crystalline solid is difficult to establish.

This history has convinced us that the elementary strategy of pasting together readily available paramagnetic building blocks and linkers should be abandoned and new components should be designed from the ground up. The opening question, then, is what features would characterize ideal organic paramagnetic building blocks for assembly into magnetic materials via metal cation complexation?

(i) Network topology: A primary characteristic must be the ability to form ordered solids with the topological requirements of a ferromagnet. The envisioned self-assembly of such building blocks and metal cations must lead to 2- or 3-D infinite networks, which are able to propagate strong magnetic interactions of the desired sign.

(ii) Conformational definition: Beyond being imaginable, the intended assemblies must have a reasonably high probability of formation. This implies that the molecular conformations and geometries of coordination foreseen for the building blocks in their target networks should, as much as possible, be structurally predetermined.

(iii) Strong intermolecular coupling: Electrostatics is a powerful force that may be exploited to guide self-assembly of magnetic solids. The presence of negative charge on the organic paramagnetic subunit should maximize its interaction with the metal cation and the consequent formation of organometallic networks with strong magnetic coupling. Use of charged components also offers control of the material’s stoichiometry.

(iv) Tunability: An attractive feature of molecule-based magnets would be control over the energy difference between

---

* To whom correspondence should be addressed.

† Current address: “Sulima-Max” Sp. z o.o., Esperanto 14a/26, 01-049 Warszawa, Poland.

[1] (a) Schlenk, W.; Brauns, M. *Chem. Ber.* **1915**, *48*, 661. (b). *Diradicals*; Borden, W. T., Ed.; Wiley: New York, 1982. (c) Berson, J. A. In *The Chemistry of Quinonoid Compounds*; Patai, S., Rappoport, Z., Eds.; Wiley: New York, 1988; Vol. 2, pp 455−536.

[2] (a) Iwamura, H. *Pure Appl. Chem.* **1987**, *59*, 1595. (b) Rajca, A. *Chem. Rev.* **1994**, *94*, 871.

[3] (a) Kahn, O. *Molecular magnetism*; Vch: New York, 1993. (b) Miller, J. S.; Epstein, A. J. *Angew. Chem., Int. Ed. Engl.* **1994**, *33*, 385. (c) Gatteschi, D. *Adv. Mater.* **1994**, *6*, 635. (d) Lahti, P. M. *Magnetic properties of organic materials;* Marcel Dekker: New York, 1999.

[4] (a) Caneschi, A.; Gatteschi, D.; Sessoli, R.; Rey, P. *Acc. Chem. Res.* **1989**, *22*, 392. (b) Caneschi, A.; Gatteschi, D.; Rey, P. In *Progress in Inorganic Chemistry*; Karlin K. D., Ed.; Wiley: New York, 1991; Vol. 39, pp 331−429.

[5] (a) Stumpf, H. O.; Ouahab, L.; Pei, Y.; Grandjean, D.; Kahn, O. *Science* **1993**, *261*, 447. (b) Stumpf, H. O.; Ouahab, L.; Pei, Y.; Bergerat, P.; Kahn, O. *J. Am. Chem. Soc.* **1994**, *116*, 3866. (c) Fegy, K.; Luneau, D.; Ohm, T.; Paulsen, C.; Rey, P. *Angew. Chem., Int. Ed. Engl.* **1998**, *37*, 1270. (d) Iwamura, H.; Inoue, K.; Hayamizu, T. *Pure Appl. Chem.* **1996**, *68*, 243. (e) Inoue, K.; Hayamizu, T.; Iwamura, H.; Hashizume, D.; Ohashi, Y. *J. Am. Chem. Soc.* **1996**, *118*, 1803. (f) Markosyan, A. S.; Hayamizu, T.; Iwamura, H.; Inoue, K. *J. Phys.-Condens. Matter* **1998**, *10*, 2323. (g) Miller, J. S.; Epstein, A. J. *J. Chem. Soc., Chem. Commun.* **1998**, 1319. (h) Zhang, J.; Ensling, J.; Ksenofontov, V.; Gutlich, P.; Epstein, A. J.; Miller, J. S. *Angew. Chem., Int. Ed. Engl.* **1998**, *37*, 657. (i) Miller, J. S.; Calabrese, J. C.; Harlow, R. L.; Dixon, D. A.; Zhang, J. H.; Reiff, W. M.; Chittipeddi, S.; Selover, M. A.; Epstein, A. J. *J. Am. Chem. Soc.* **1990**, *112*, 5496.

[6] (a) Misiołek, A.; Huang, R.; Kahr, B.; Jackson, J. E. *J. Chem. Soc., Chem. Commun.* **1996**, 2119. (b) Stoudt, S. J.; Gopalan, P.; Bakulin, A.; Kahr, B.; Jackson, J. E. *Inorg. Chem.* **1996**, *35*, 6614.

10.1021/ja0021417 CCC: $20.00

singly occupied frontier molecular orbitals (SOMOs) and the resulting magnitude and sign of the intramolecular electron coupling of the polyradical subunits. Besides the importance and challenge of this aim for assembly of organic based ferromagnetic substances, tuning of this splitting close to zero is expected to produce interesting materials with other than magnetic properties.[7]

(v) Variable spin content: Polyradical building blocks are not necessarily optimal for all molecular magnet syntheses. Many polyradicals are low-spin coupled or have only a weak preference for a high-spin ground state. For the preparation of magnets, monoradicals that can be strongly coupled by ion binding offer an alternative synthesis motif. With their small spin values, monoradicals could also make better partners for high-spin transition metal cations in the assembly of ferrimagnets. The ideal solution appears to be a unit which, depending on the strategy desired, would have the ability to carry one, two, or a higher number of controllably coupled electrons.

(vi) Compactness: The two- or three-dimensionality of the target networks required for ferromagnet synthesis implies the presence of void spaces between structurally active elements. The bigger these cavities are, the less likely they are to form. Ideal building blocks should therefore be as compact as possible, maximizing the unpaired electron density and the resulting inter- and, in the case of polyradicals, intramolecular spin−spin interactions.

(vii) Kinetic stability: The molecular frame of such building blocks must be stable enough for practical handling and assembly into the targeted networks. It must tolerate ambient temperatures and ordinary solvents and, in the ideal case, would also be unperturbed by exposure to air or water.

A common approach to the design of building blocks as described above is to replace sp^2 radical carbons of non-Kekule hydrocarbons with other spin-bearing units.[2b,8] Despite its simplicity, this method has successfully yielded many triplet state molecules and anions.[9] We now extend this strategy to another non-Kekule hydrocarbon: dimethylenecyclobutadiene[10,11] (**DMCB**, Figure 1). To replace the secondary sp^2 CH$^\bullet$ radical sites in **DMCB**, we selected the semidione radical anion fragment $(C_2O_2)^{\bullet-}$. This choice was based on its negative charge and ion binding ability and on the calculated closeness between the one-electron energies of the $(C_2O_2{}^{\bullet-})$ and CH$^\bullet$ SOMOs, as well as their congruent orbital topologies. Despite this drastic structural modification, the frontier orbitals **A** and **B** (see Figure 1) of the newly obtained dianion **1**$^{2-}$ retain the desired near degeneracy of their orbital parents in **DMCB** (**a** and **b**), as shown by preliminary Hückel calculations. Since the new pair of frontier orbitals also retain the nondisjoint character of **a** and **b**, **1**$^{2-}$ (if stable) appears reasonably likely to have a triplet ground state. Available structural precedents indicate that 2-D ferromagnetically coupled honeycomb networks (Figure 2) should be formed by crystallization of M^{3+} salts of **1**$^{2-}$. Such networks are formed by derivatives of dihydroxybenzoquinone (**2**$^{2-}$),[12] a closed shell structural analogue to dianion **1**$^{2-}$. Moreover, the symmetrical octahedral coordination spheres of the trischelated metal cations should also ensure high-spin coupling between the organic paramagnetic subunits coordinated

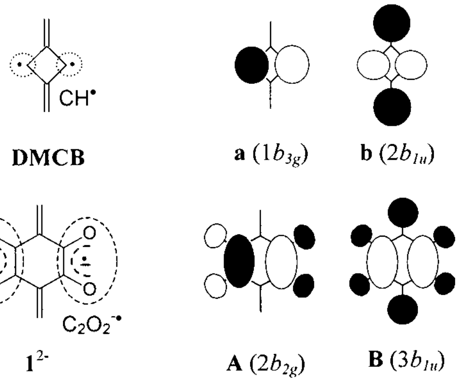

Figure 1. Frontier orbitals of **DMCB** and **1**$^{2-}$.

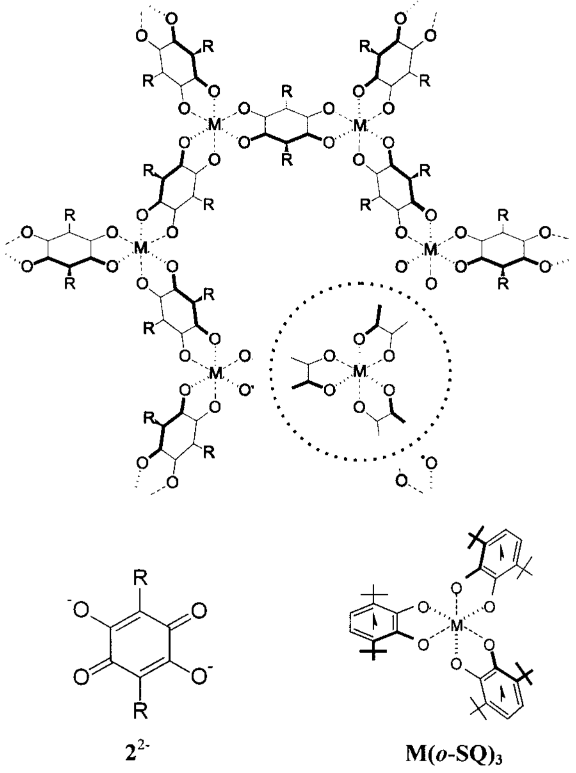

Figure 2. Idealized target honeycomb structures made of anions of **1** and metal cations resembling those reported for salts of dihydroxyquinone (**2**$^{2-}$). The symmetry of their coordination sites (circled in the picture) is similar to that of high-spin coupled semiquinone complexes of Al^{3+} and Ga^{3+} (**(o-SQ)$_3$M**).

---

(7) Berson, J. A. *Acc. Chem. Res.* **1997**, *30*, 238.

(8) Dougherty, D. A. *Acc. Chem. Res.* **1991**, *24*, 88.

(9) Derivatives of *m*-xylylene: (a) Ishida, T.; Iwamura, H. *J. Am. Chem. Soc.* **1991**, *113*, 4238. (b) Veciana, J.; Rovira, C.; Crespo, M. I.; Armet, O.; Domingo, V. M.; Palacio, F. *J. Am. Chem. Soc.* **1991**, *113*, 2552. (c) Shiomi, D.; Tamura, M.; Sawa, H.; Kato, R.; Kinoshita, M. *J. Phys. Soc. Jpn.* **1993**, *62*, 289. (d) Kanno, F.; Inoue, K.; Koga, N.; Iwamura, H. *J. Phys. Chem.* **1993**, *97*, 13267. (e) Okada, K.; Matsumoto, K.; Oda, M.; Murai, H.; Akiyama, K.; Ikegami, Y. *Tetrahedron Lett.* **1995**, *36*, 6689. (f) Rajca, A.; Rajca, S.; Desai, S. R. *J. Chem. Soc., Chem. Commun.* **1995**, 1957. (g) Shultz, D. A.; Boal, A. K.; Driscoll, D. J.; Kitchin, J. R.; Tew, G. N. *J. Org. Chem.* **1995**, *60*, 3578. (h) Wienk, M. M.; Janssen, R. A. J. *J. Am. Chem. Soc.* **1996**, *118*, 10626. (i) Yano, M.; Sato, K.; Shiomi, D.; Ichimura, A.; Abe, K.; Takui, T.; Itoh, K. *Tetrahedron Lett.* **1996**, *37*, 9207. (j) Okada, K.; Matsumoto, K.; Oda, M.; Akiyama, K.; Ikegami, Y. *Tetrahedron Lett.* **1997**, *38*, 6007. (k) Wienk, M. M.; Janssen, R. A. J. *J. Am. Chem. Soc.* **1997**, *119*, 5398. (l) Okada, K.; Imakura, T.; Oda, M.; Kajiwara, A.; Kamachi, M.; Yamaguchi, M. *J. Am. Chem. Soc.* **1997**, *119*, 5740. (m) Tanaka, M.; Matsuda, K.; Itoh, T.; Iwamura, H. *J. Am. Chem. Soc.* **1998**, *120*, 7168. (n) Shultz, D. A.; Farmer, G. T. *J. Org. Chem.* **1998**, *63*, 6254. (o) Ito, A.; Taniguchi, A.; Yamabe, T.; Tanaka, K. *Org. Lett.* **1999**, *1*, 741. Derivatives of trimethylenemethane: (p) Shultz, D. A.; Boal, A. K.; Lee, H.; Farmer, G. T. *J. Org. Chem.* **1999**, *64*, 4386. (q) Shultz, D. A.; Boal, A. K.; Farmer, G. T. *J. Org. Chem.* **1998**, *63*, 9462. (r) Shultz, D. A.; Boal, A. K.; Farmer, G. T. *J. Am. Chem. Soc.* **1997**, *119*, 3846.

(10) (a) Dowd, P.; Paik, Y. H. *J. Am. Chem. Soc.* **1986**, *108*, 2788. (b) Snyder, G. J.; Dougherty, D. A. *J. Am. Chem. Soc.* **1989**, *111*, 3927.

(11) Du, P.; Hrovat, D. A.; Borden, W. T. *J. Am. Chem. Soc.* **1989**, *111*, 3773.

(12) Weiss, A.; Riegler, E.; Robl, C. *Z. Naturforsch. (B)* **1986**, *41*, 1501.

to them, as demonstrated by the quartet ground states observed for the analogous gallium and aluminum complexes of *o*-semiquinones (Figure 2).[13] Use of such diamagnetic tripositive cations with $\mathbf{1}^{2-}$ would lead to net internal electrostatic balance. But the idea of such self-assembly may also be extended to monoanions $\mathbf{1}^{\bullet-}$. In this case, honeycomb nets could achieve neutrality only if additional counterions were included or if alternating metal cations of different charges (+1 and +2) were incorporated into neighboring sites. Similar charge balancing strategies have been used for preparation of ferrimagnetic honeycomb structures with oxalate anions as the magnetic coupling elements between spin-bearing transition metal ions.[14] The paramagnetic organic component $\mathbf{1}^{2-}$ (or $\mathbf{1}^{-}$) in place of diamagnetic oxalate dianion should considerably strengthen such interactions, leading to higher T_c values.

Theoretical Studies of $\mathbf{1}^{2-}$ and Its Derivatives. An understanding of the relationship between electronic properties and structural modifications of $\mathbf{1}^{2-}$ should enable the design of electronically "tuned" derivatives, optimized for assembly of molecular magnets. Specifically, the tuning should favor a high-spin ground state. We have therefore studied $\mathbf{1}^{2-}$ and its derivatives using ab initio MCSCF wave functions and focusing on the correlation between structural modifications and the magnitude and sign of $\Delta E_{(S-T)}$ (the singlet−triplet energy difference). We also have explored the general assumption that the value of $\Delta E_{(S-T)}$ should be maximal when the frontier orbitals are energetically degenerate (providing that the spatial overlap remains relatively unperturbed by such modifications).

The most straightforward and computationally tractable modifications of $\mathbf{1}^{2-}$ are (a) coordination of the semidione units to different metal cations and (b) replacement of the hydrogen atoms with other substituents. The set of species used in ab initio studies of the S−T gap includes "naked" dianion $\mathbf{1}^{2-}$ and its symmetrical complexes $\mathbf{1}(MF_n)_2$ with metal cations of increasing charge (M = Li^+, Be^{2+}, Al^{3+} with n = 0, 1, and 2, respectively; in the latter two systems, the fluoride anions were added to balance the charge, keeping the overall complexes neutral). A series of lithium complexes was also chosen to assess the effects of adding substituents such as fluorine ($F_4\mathbf{1}Li_2$) and hydroxy groups ($(OH)_4\mathbf{1}Li_2$) (Figure 3). Calculations on the parent **DMCB** hydrocarbon diradical were also performed. CAS-MCSCF (complete active space multiconfigurational self-consisted field) calculations correlating electrons in the π orbital space were run at the following levels of theory: CAS(2,2), CAS(2,3), and CAS(14,12) for derivatives of $\mathbf{1}^{2-}$ and CAS(2,2) and CAS(6,6) for **DMCB**. In the notation CAS(N,M) the N and M values indicate numbers of electrons and orbitals in the CAS calculations. The most extensive active space included all valence π electrons and π orbitals, whose manifold may be derived starting from the well-known π orbital diagram of benzene. Figure 4 presents energies of the molecular orbitals of benzene, $\mathbf{3}^{2-}$ (the D_{6h} rhodizonic acid dianion), and $\mathbf{1}^{2-}$ as calculated by use of the Hückel method.[15] Each of the six benzene π orbitals can be mapped to two orbitals of $\mathbf{3}^{2-}$ composed, in turn, of C═O π and π^* fragment orbitals. Both have the same transverse nodal planes as the parent benzene orbital but the higher energy orbital also includes a radial node going around the molecule between the carbon and oxygen atoms. Since the lowest orbital with a radial node has higher energy then the highest one without it, two distinct, six-orbital subsets are formed, preserving the orbital pattern of benzene.

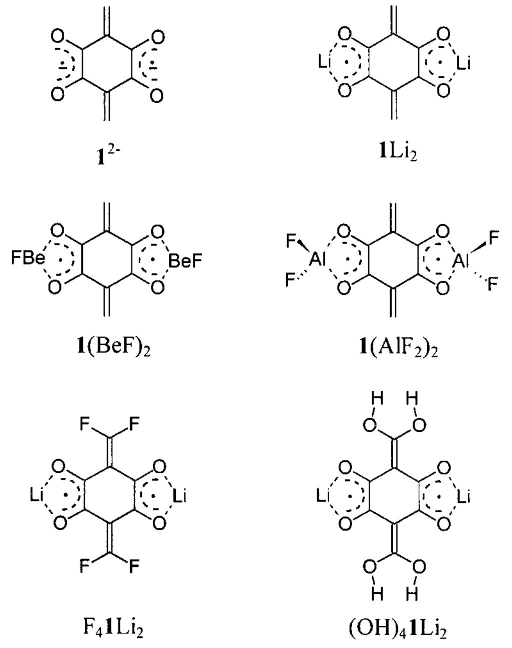

Figure 3. Species investigated in the present study.

Formal replacement of the two carbonyl oxygens at the 1 and 4 positions of $\mathbf{3}^{2-}$ with sp^2 methylene groups produces $\mathbf{1}^{2-}$. Of the two degenerate LUMOs of $\mathbf{3}^{2-}$, one has a nodal plane through the 1 and 4 positions and thus has zero coefficients on the external methylene carbon atoms; this relatively unperturbed orbital becomes **A** in $\mathbf{1}^{2-}$. But the HOMO of $\mathbf{3}^{2-}$, with its substantial contributions from the modified sites, rises in energy to become **B**. The magnitude of this shift has a value close to the HOMO/LUMO gap in $\mathbf{3}^{2-}$ so that orbitals **A** and **B** in $\mathbf{1}^{2-}$ are almost degenerate. Meanwhile, the second LUMO in $\mathbf{3}^{2-}$, originally degenerate with **A**, rises even more than did **B**, placing its energy well above that of **A** and **B**, and leaving the latter two as the clearly expected SOMOs (or HOMO/LUMO pair). Analogous perturbations are also seen for the other π orbitals.

Results

Table 1 summarizes the energy splittings ($\Delta E_{(S-T)}$) between the lowest lying singlet and triplet states for the species in this work. Reported gaps represent structures optimized in D_{2h} symmetry at the indicated computational level, except for the CAS(14,12)/6-31+G* values which were computed by using the CAS(14,12)/6-31G* geometries. These energies are expressed in kcal/mol as are the ZPE corrections calculated at the CAS(2,2)/6-31G* level. In most cases calculations found ^1A_g and $^3B_{3u}$ to be the lowest lying singlet and triplet electronic states, respectively. The only exception was the naked dianion $\mathbf{1}^{2-}$ whose $^3B_{2u}$ ($|...2b_{3g}{}^2 3b_{1u}{}^1 3b_{3g}{}^1\rangle$) state was found to be 0.2 kcal/mol below $^3B_{3u}$ ($|...2b_{3g}{}^2 3b_{1u}{}^1 2b_{2g}{}^1\rangle$). To keep all the comparisons consistent, however, all orbital populations and geometry analyses for $\mathbf{1}^{2-}$ and congeners (Tables 3 and 4) were based on the $^3B_{3u}$ state. Figure 5 graphically depicts the ($\Delta E_{(S-T)}$) gaps as a function of $\Delta E_{(B-A)}$, the difference between the one-electron energies of the singly occupied frontier orbitals

---

[13] Lange, C. W.; Conklin, B. J.; Pierpont, C. G. *Inorg. Chem.* **1994**, *33*, 1276.

[14] (a) Tamaki, H.; Zhong, Z. J.; Matsumoto, N.; Kida, S.; Koikawa, M.; Achiwa, N.; Hashimoto, Y.; Okawa, H. *J. Am. Chem. Soc.* **1992**, *114*, 6974. (b) Ohba, M.; Tamaki, H.; Matsumoto, N.; Okawa, H. *Inorg. Chem.* **1993**, *32*, 5385. (c) Okawa, H.; Matsumoto, N.; Tamaki, H.; Ohba, M. **1993**, *232*, 617. (d) Decurtins, S.; Schmalle, H. W.; Oswald, H. R.; Linden, A.; Ensling, J.; Gutlich, P.; Hauser, A. *Inorg. Chim. Acta* **1994**, *216*, 65.

[15] Calculations were performed on a Power MacIntosh 7200/90 with use of the program HMO 1.1 by Allan Wissner (resonance integrals (C−C)−1, (C−O)−1.06; Coulomb integrals C−0, O−0.97).

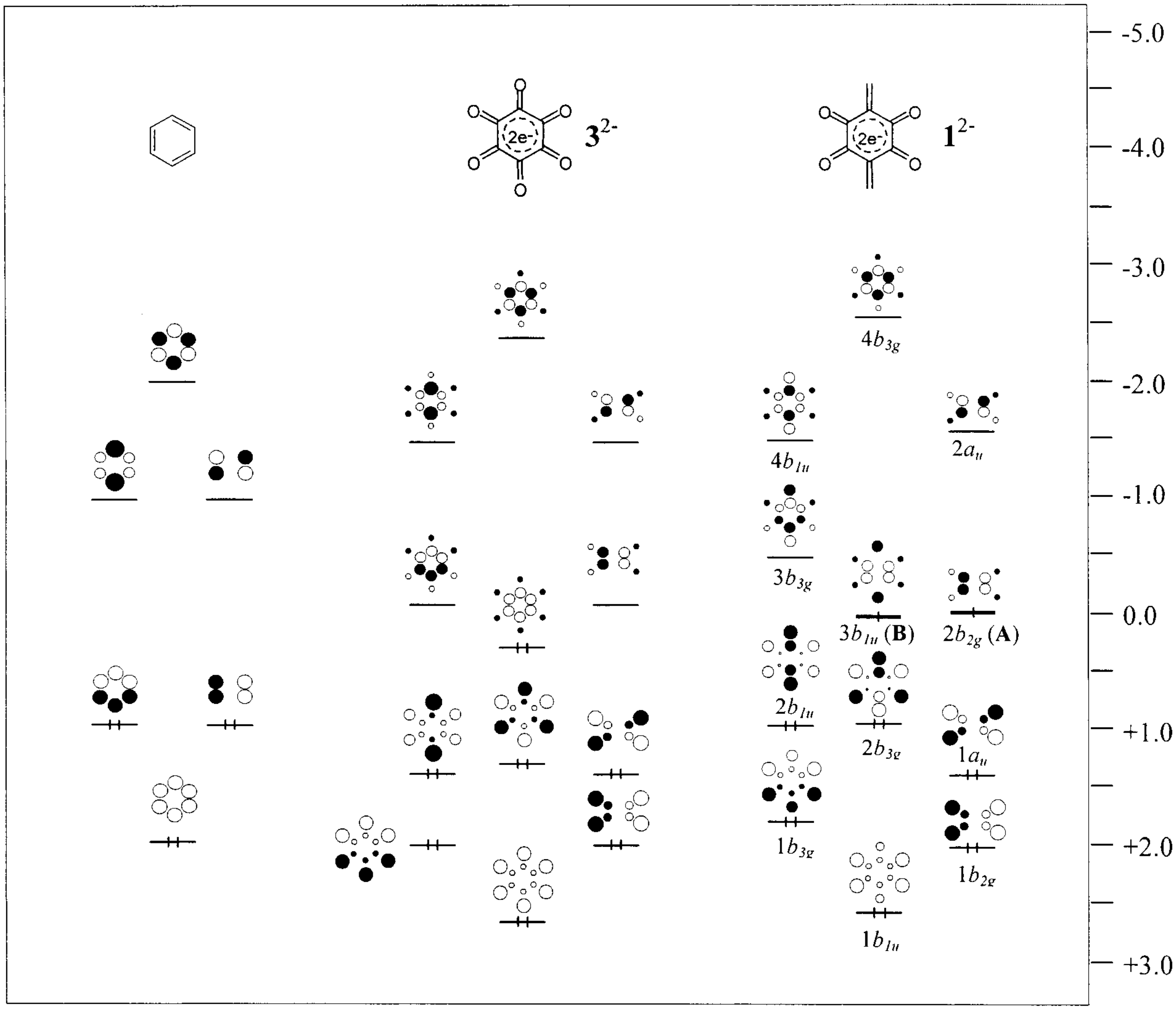

Figure 4. Diagram of the π orbitals of benzene, rhodizonic acid dianion ($\mathbf{3}^{2-}$), and $\mathbf{1}^{2-}$. Energy levels shown were obtained using the Hückel method.

Table 1. Singlet−Triplet Energy Splittings ($\Delta E_{(S-T)}$) and Zero-Point Energies (ZPEs) for the Investigated Complexes in their Lowest Singlet (^1A_g) and Triplet ($^3B_{3u}$) Electronic States, as Calculated at the Indicated Levels

level of theory/6-31G*	$\mathbf{1}^{2-}$	$\mathbf{1}Li_2$	$\mathbf{1}(BeF)_2$	$\mathbf{1}(AlF_2)_2$	$F_4\mathbf{1}Li_2$	$(OH)_4\mathbf{1}Li_2$	DMCB
CAS(2,2)	−5.7	1.8	4.4	4.9	3.7	3.9	7.2
$ZPE_{CAS(2,2)}$	−0.6	−0.1	0.0	0.0	−0.1	0.1	0.4
CAS(2,3)/(2,2)	−9.4	0.1	3.2	3.9	2.9	3.5	
CAS(14,12)	−12.6 −12.4[a]	−0.5	3.8	4.8	2.4	4.8	19.8[b]
CAS(14,12)/6-31+G*	−17.3	−2.0	3.2	4.3	1.5	4.5	17.7[b]

[a] $^3B_{2u}$ state. [b] For **DMCB**, CAS(6,6) wave functions were used to span the full π space.

Table 2. Values of $\Delta E_{(B-A)}$ and Occupancies of Orbitals A and B in the TCSCF Singlet Wave Functions

	$\Delta E_{(B-A)}$ ROHF (hartree)	occup.TCSCF	
		B	A
$\mathbf{1}^{2-}$	0.0453	1.59	0.41
$\mathbf{1}Li_2$	0.0209	1.34	0.66
$\mathbf{1}(BeF)_2$	0.0091	1.19	0.81
$\mathbf{1}(AlF_2)_2$	0.0041	1.11	0.89
$F_4\mathbf{1}Li_2$	0.0043	1.08	0.92
$(OH)_4\mathbf{1}Li_2$	−0.0112	0.78	1.22
DMCB	0.0338	1.53	0.47

B and **A** in the ROHF triplets. The $\Delta E_{(B-A)}$ values and occupancies of **A** and **B** in the TCSCF (CAS(2,2)) singlet wave functions are presented in Table 2.

Tables 3 and 4 list the occupancies of the π (active) orbitals in the CAS(14,12) wave functions for the ^1A_g and $^3B_{3u}$ states, together with the CAS(2,3) results for ^1A_g. Table 5 contains selected bond lengths; Cartesian coordinates of the unique atoms and vibrational frequencies in all calculated complexes may be found in the Supporting Information.

Discussion

Series a: Effect of Metal Cation Coordination. Electrostatic interactions of electrons with metal cations should lower the energies of all occupied MOs. Orbitals concentrated close to the cations should, however, be affected more strongly then those further away. With substantial density on the methylene carbons, orbital **B** ($3b_{1u}$) does not interact with the cations as strongly as orbital **A** ($2b_{2g}$), which is distributed only on the

Table 3. Occupancies of the Active Orbitals of Investigated Complexes in the Singlet ^1A_g CAS(14,12) and CAS(2,3) Wave Functions

orbital	$\mathbf{1}^{2-}$	$\mathbf{1}Li_2$	$\mathbf{1}(BeF)_2$	$\mathbf{1}(AlF_2)_2$	$F_4\mathbf{1}Li_2$	$(OH)_4\mathbf{1}Li_2$
$1b_{1u}$	1.98	1.98	1.99	1.99	1.98	1.99
$1b_{2g}$	1.96	1.98	1.98	1.99	1.98	1.98
$1b_{3g}$	1.97	1.97	1.98	1.99	1.98	1.98
$1a_u$	1.95	1.97	1.98	1.99	1.97	1.98
$2b_{1u}$	1.92	1.91	1.91	1.92	1.92	1.93
$2b_{3g}$	1.94	1.92	1.92	1.92	1.93	1.94
$3b_{1u}$ **B**	1.66[a]	1.41[a]	1.25[a]	1.17[a]	1.14[a]	0.82[a]
	1.68	1.56	1.44	1.26	1.37	1.20
$2b_{2g}$ **A**	0.28[a]	0.58[a]	0.74[a]	0.82[a]	0.86[a]	1.18[a]
	0.17	0.40	0.53	0.73	0.62	0.80
$3b_{3g}$	0.06[a]	0.02[a]	0.01[a]	0.01[a]	0.01[a]	0.00[a]
	0.29	0.17	0.15	0.12	0.12	0.09
$4b_{1u}$	0.05	0.03	0.03	0.02	0.03	0.03
$2a_u$	0.05	0.07	0.07	0.06	0.06	0.06
$4b_{3g}$	0.03	0.03	0.02	0.01	0.03	0.02

[a] CAS(2,3).

Table 4. Occupancies of the Active Orbitals of Investigated Complexes in the Triplet $^3B_{3u}$ CAS(14,12) Wave Functions

orbital	$\mathbf{1}^{2-}$	$\mathbf{1}Li_2$	$\mathbf{1}(BeF)_2$	$\mathbf{1}(AlF_2)_2$	$F_4\mathbf{1}Li_2$	$(OH)_4\mathbf{1}Li_2$
$1b_{1u}$	1.98	1.99	1.99	1.99	1.99	1.99
$1b_{2g}$	1.98	1.99	1.99	1.99	1.99	1.99
$1b_{3g}$	1.96	1.98	1.98	1.98	1.98	1.98
$1a_u$	1.96	1.98	1.98	1.98	1.98	1.98
$2b_{1u}$	1.91	1.92	1.92	1.93	1.93	1.94
$2b_{3g}$	1.91	1.90	1.90	1.90	1.93	1.93
$3b_{1u}$ **B**	1.02	1.01	1.00	1.00	1.00	1.00
$2b_{2g}$ **A**	1.01	1.01	1.01	1.00	1.01	1.01
$3b_{3g}$	0.11	0.11	0.11	0.11	0.08	0.08
$4b_{1u}$	0.04	0.03	0.03	0.03	0.03	0.03
$2a_u$	0.07	0.07	0.07	0.07	0.06	0.06
$4b_{3g}$	0.03	0.02	0.02	0.02	0.02	0.02

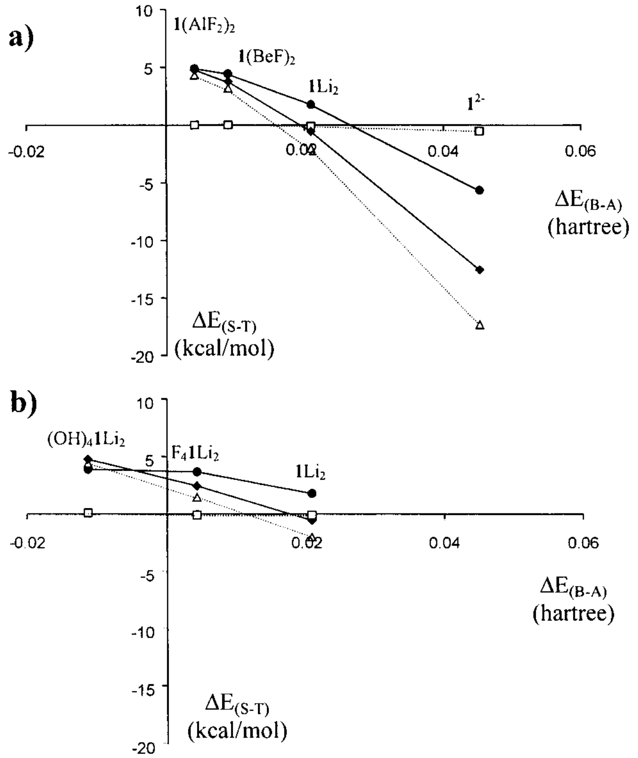

Figure 5. S−T gaps calculated for (a) $\mathbf{1}^{2-}$ complexed by different metal cations and (b) $\mathbf{1}Li_2$ with different substituents R vs $-\Delta E_{(B-A)}$ at (●) CAS(2,2)/6-31G*, (◆) CAS(14,12)/6-31G*, and (△) CAS(14,12)/6-31+G* levels of the theory. (□) Zero-point corrections at the CAS-(2,2) level.

semidione units (Figure 1). These disparate interactions lead to a decrease in the gap between **A** and **B** ($\Delta E_{(B-A)}$) as the cation charge increases; $\Delta E_{(A-B)}$ drops from 0.0453 through 0.0209 and 0.0091, to 0.0041 hartree for $\mathbf{1}^{2-}$, $\mathbf{1}Li_2$, $\mathbf{1}(BeF)_2$, and $\mathbf{1}(AlF_2)_2$, respectively. The values of $\Delta E_{(A-B)}$ are obtained at the single configuration ROHF level of theory, so their physical relevance to the CAS results is approximate. Nonetheless, a correlation between $\Delta E_{(A-B)}$ values and S−T gaps is expected, and indeed an increasing preference for the triplet state tracks the shrinking interorbital gap. At the CAS(2,2) level of theory the ground state of $\mathbf{1}^{2-}$ is a singlet lying 5.7 kcal/mol below the triplet; for $\mathbf{1}Li_2$ the singlet already lies above the triplet by 1.8 kcal/mol, while for $\mathbf{1}(BeF)_2$ and $\mathbf{1}(AlF_2)_2$ this value increases to 4.4 and 4.9 kcal/mol, respectively. Extrapolation of the curve obtained leads to a predicted triplet preference of about 5 kcal/mol for $\Delta E_{(A-B)} = 0$. At the current level of theory, this value is probably close to the maximum achievable by tuning of the relative energies of the orbitals.

Series b: Effect of Substitution. Unlike **B,** orbital **A** has zero coefficients on the exocyclic methylene carbons in $\mathbf{1}^{2-}$. Replacement of the hydrogen atoms with other substituents should thus affect the energy of **B** much more than that of **A**. Since orbital **B** lies lower than **A**, the desired decrease of the **A**−**B** gap should be achieved by substitution of $\mathbf{1}^{2-}$ with electron-donating groups. Figure 5b shows the effect of such structural modifications. Fluorine, a weak π donor, already has a substantial effect, lowering $\Delta E_{(B-A)}$ from 0.0209 hartree for H-substituted $\mathbf{1}Li_2$ to 0.0043 hartree for $F_4\mathbf{1}Li_2$. The effect of the more strongly donating hydroxy groups is powerful enough to reverse the HOMO-LUMO orbital order ($\Delta E_{(A-B)} = -0.0112$ hartree). Although in both cases a strong preference for the triplet follows, the $\Delta E_{(S-T)} \sim \Delta E_{(A-B)}$ correlation cannot be directly related to that obtained in series a. For example, complexes $\mathbf{1}(AlF_2)_2$ and $F_4\mathbf{1}Li_2$ have almost the same values for $\Delta E_{(A-B)}$ (0.0041 vs 0.0043 hartree) but somewhat different $\Delta E_{(S-T)}$ values (4.9 vs 3.7 kcal/mol). Inspection of the MO coefficients confirms that replacement of hydrogens with heavy atoms causes more extensive delocalization of orbital **B** and lowers its spatial overlap with **A**. This in turn weakens the electrostatic interactions between the frontier orbitals and slightly lowers the triplet preference. The calculated HOMO-LUMO gap is larger for the model **DMCB** (0.0338 hartree) than for $\mathbf{1}Li_2$. Nonetheless, its triplet preference at the CAS(2,2) level of theory is the highest of all the investigated species (7.2 kcal/mol). In this case the electrostatic interactions between the frontier electrons must by magnified by the small size and resulting strong spatial overlap of the two SOMOs.

Correlation Effects. Examination of results obtained at the CAS(14,12) level of theory shows that the correlation energy corrections for the calculated species depend on their structures. The more charged are the cations coordinated to $\mathbf{1}^{2-}$, the lower is the magnitude of ($E_{CAS(2,2)} - E_{CAS(14,12)}$) for both singlet and triplet states. Apparently, with increasing charge of the coordinated cation, the bonding electrons of the π system localize more on the carbonyl oxygens while the antibonding frontier electrons localize on the carbons, weakening their mutual interactions. Coordination also increases the gap between bonding and antibonding orbitals leading to lower polarizability (i.e. higher excitation energies) in the π system. Stabilization of the singlet drops faster than for the triplet. Thus, the improvement in correlation description favors singlet versus triplet by 6.9 kcal/mol for $\mathbf{1}^{2-}$, the first member of series a, but by only 0.1 kcal/mol for $\mathbf{1}(AlF_2)_2$, the last member. A similar tendency is observed for the substituent effects in series b (2.3 kcal for $\mathbf{1}Li_2$

Table 5. Selected Bond Lengths (in Å) of $\mathbf{1}^{2-}$ and Its Complexes Optimized at the CAS(14,12)/6-31G* Level

	a($^3B_{3u}$)	**a**(^1A_g)	**b**($^3B_{3u}$)	**b**(^1A_g)	**c**($^3B_{3u}$)	**c**(^1A_g)	**d**($^3B_{3u}$)	**d**(^1A_g)
$\mathbf{1}^{2-}$	1.436	1.487	1.501	1.457	1.356	1.383	1.252	1.240
$\mathbf{1}Li_2$	1.431	1.451	1.473	1.461	1.357	1.357	1.263	1.257
$\mathbf{1}(BeF)_2$	1.423	1.437	1.457	1.458	1.358	1.351	1.269	1.264
$\mathbf{1}(AlF_2)_2$	1.423	1.433	1.457	1.461	1.358	1.349	1.271	1.266
$F_4\mathbf{1}Li_2$	1.439	1.441	1.471	1.478	1.366	1.356	1.263	1.261
$(OH)_4\mathbf{1}Li_2$	1.433	1.441	1.474	1.474	1.351	1.345	1.259	1.256

vs −0.9 for $(OH)_4\mathbf{1}Li_2$). One of the factors contributing to this covariation may be the fact that leveling of the HOMO-LUMO gap results in singlets having more diradical and less ionic character, but it has no analogous effect on triplets. Since correlation generally favors more ionic wave functions,[16] the relative stabilization by correlation of the singlet vs the triplet thus decreases.

Especially impressive is the relative stabilization of the triplet state in the case of the model **DMCB**, where the triplet preference rises from 7.2 for CAS(2,2) to 19.8 kcal/mol for CAS(6,6). Additional configuration interaction (CI) corrections due to all p single and double (π-SD) and all σ-S, π-SD excitations from the CAS multireference wave function were reported to yield preferences of 20.2 and 18.2 kcal/mol, respectively.[11] The authors attributed these large corrections to a higher degree of delocalization of the frontier electrons in the triplet compared to the singlet and their resulting stronger interaction with other electrons. The second value reflects the correlation of π with σ electrons, which usually provides extra stabilization for singlets. Unfortunately, the species described herein were too large for such studies via CASPT2N or MR SD CI methods with the software available to us.

Examination of the partial occupancies of the active orbitals in the CAS(14,12) wave functions of both singlet and triplet states (Tables 3 and 4) shows high occupation of $3b_{3g}$, especially for $\mathbf{1}^{2-}$. For this dianion, a triplet state of different symmetry, $^3B_{2u}$ ($|...2b_{3g}{}^2 3b_{1u}{}^1 3b_{3g}{}^1\rangle$), is slightly lower in energy than the $^3B_{3u}$ ($|...2b_{3g}{}^2 3b_{1u}{}^1 2b_{2g}{}^1\rangle$) state. In this doubly charged situation, the low-lying $3b_{3g}$ orbital could be electrostatically preferred over **A** ($2b_{2g}$), due to the more disjoint relationship of **B** and $3b_{3g}$, than of **B** and **A**. The less complete CAS(2,3) (**B**, **A**, $3b_{3g}$ and 2 frontier electrons) calculations, however, show rather low populations of $3b_{3g}$, indicating that in the full π space, it is mostly excitations from orbitals other than **A** and **B** that fill this orbital.

To describe more accurately the anionic character of the organic core $\mathbf{1}^{2-}$ of the species studied here, single point CAS(14,12) calculations with the 6-31+G* basis set were performed on the geometries optimized at the CAS(14,12)/6-31G* level. Addition of the diffuse "+" sets of s and p functions on heavy atoms generally favors singlets. The corrections, however, are not dramatic (see Table 1), and as expected, they decrease with tighter coordination of the metal ions.

Molecular Geometry. Potential degeneracy in nondisjoint frontier orbitals does not necessarily ensure that a molecule will have a triplet ground state. The degeneracy may be lifted by Jahn−Teller distortion. For example, lowering of the symmetry from 3-fold or higher to pseudo-D_{2h} stabilizes singlet states of 4nπ electron "antiaromatic" annulenes.[17,18] In the present systems evidence for such distortions was sought at the CAS(2,2) level by vibrational analysis of the D_{2h} optimized structures.

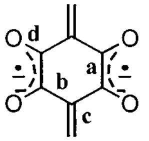

Figure 6. Labeling scheme for bond lengths listed in Table 5.

All frequency values for series a ($\mathbf{1}^{2-}$, $\mathbf{1}Li_2$, $\mathbf{1}(BeF)_2$, and $\mathbf{1}(AlF_2)_2$) turned out to be real in both singlet and triplet states. Values for some modes of bending out of plane were however very low, showing that the planar geometry is a rather shallow minimum. This finding is not surprising, in light of the nonplanar geometries we have found for the neutral tetraketone, both computationally and experimentally (with Ph substituents).

In series b, for triplet state $F_4\mathbf{1}Li_2$ all the frequencies are real, while there is one (16 cm^{-1}) imaginary mode for the singlet state. For $(OH)_4\mathbf{1}Li_2$, there are three imaginary frequencies for each state. Two of them in each state (426, 425 cm^{-1} (s) and 458, 457 cm^{-1} (t)) belong to combinations of out-of-plane torsions of the hydrogens of the OH groups. The third one (18 cm^{-1}(s) and 23 cm^{-1}(t)), like the imaginary frequency of singlet state $F_4\mathbf{1}Li_2$, represents boatlike out-of-plane bending of the molecular frame. Presumably these distortions arise from the steric interactions introduced when H is replaced by the larger F and OH groups.

While OH torsions may easily be attributed to the artificially high D_{2h} symmetry chosen for the molecules, bending of the whole molecule must reflect an intrinsic characteristic. Does it indicate a tendency toward Jahn−Teller distortions or just high flexibility of the molecular frame? Optimization of singlet $F_4\mathbf{1}Li_2$ in the boatlike C_{2v} geometry obtained by following the imaginary vibration yields an energy less than 15 cal/mol lower than that in the D_{2h} form. Meanwhile, the occupation numbers of the frontier orbitals barely change (from 0.92(**A**), 1.08(**B**) to 0.91(**A**), 1.09(**B**)), suggesting that the distortion reflects steric or dipole repulsion rather than any frontier orbital effect. Whatever its nature, the out-of-plane distortion is energetically negligible compared to the S−T gap.

To probe further the flexibility of the molecular frame of $\mathbf{1}Li_2$, single point CAS(14,12) calculations on the triplet at the optimal geometry of the singlet (and vice versa) were performed. The energy of the triplet at the singlet geometry was only 1.6 kcal/mol higher than at its own optimum, but for the less forgiving singlet state molecule, the analogous increase was 2.8 kcal/mol. On the basis of the bond lengths of both singlet and triplet state complexes (Table 5), it appears that the molecular frame is best described as two semidione units connected through vinylidene bridges (Figure 6). Shortening of bond **a** and elongation of **d** with increasing charge of the coordinated cation may be understood as arising from increasing recruitment of the unpaired electron density to the semidione fragment, wherein the SOMOs are C−C bonding and C−O antibonding. Besides the previously discussed deviation from planarity of $F_4\mathbf{1}Li_2$, some bond length differences were found between singlet and triplet geometries. For singlet structures bonds **a** and **b** are longer while **c** and **d** are shorter than for the corresponding triplets.

---

[16] Borden, W. T.; Davidson, E. R. *Acc. Chem. Res.* **1996**, *29*, 67.

[17] Breslow, R. *Pure Appl. Chem.* **1982**, *54*, 927.

[18] Borden, W. T. In ref 1b, pp 1−72.

These variations can be understood in terms of the calculated shifts in electron occupancy from orbital **B** to **A**.

Conclusions

We have outlined a wish list of desirable characteristics for discrete building blocks of metal cation/radical anion-based molecular magnets. Mono- and dianions of tetrone **1** are now proposed as a new class of candidate species to satisfy those requirements. Though it is a distant relative of non-Kekule hydrocarbons, molecule $\mathbf{1}^{2-}$ may be viewed as a diradical where the degeneracy of the frontier orbitals is "accidental" (albeit intentional) rather then critically depending on the system's symmetry.

Our full π space MCSCF ab initio calculations have confirmed both the low value of the $\Delta E_{(S-T)}$ gaps for derivatives of $\mathbf{1}^{2-}$ and the intended tunability of the ground-state preference in $\mathbf{1}^{2-}$ via structural modifications. These studies predict that the coordination expected for $\mathbf{1}^{2-}$ in the target networks will strengthen the preference for the high-spin ground state, as will substitution on the vinylidene sites with electron-donating substituents. The maximum value of $\Delta E_{(S-T)}$ computed at the highest theoretical level investigated is 4.5 kcal/mol for $(OH)_4\mathbf{1}Li_2$, the most electron rich system examined. This energetic splitting, while modest, is still large compared to those within or between most previously reported organic paramagnetic building blocks for magnetic materials.

Obviously the S−T energy gaps in experimentally accessible systems will differ from those predicted above for idealized species. Because of computational limitations, only the π electrons and orbitals were included in the correlation treatment, though it is known that dynamic correlation with σ electrons may substantially change the results.[15] We found no obvious state-splitting distortion from the D_{2h} geometry imposed in the calculations, but we cannot rigorously rule out such a possibility. And of course, the molecular frame of $\mathbf{1}^{2-}$ may not be stable enough for practical handling and assembly into the targeted networks, though preliminary laboratory results suggest otherwise.

Strong intermolecular ferromagnetic spin−spin coupling is as important for the success of the outlined strategy as is the intramolecular variety. Unfortunately, extension of the calculations to such large systems was beyond our capabilities at the theoretical level employed in this work. A less computationally demanding study of the effects of metal cation relays on intermolecular spin−spin interactions is currently underway in our labs and will be described in a separate report. It is modeled on the Gatteschi group's recent analysis, using density functional theory, of a high spin coupled schiff-base diquinone radical complex of diamagnetic Ti(IV) that was validated by experimental neutron diffraction determination of the spin density map.[19a]

The expected ability of $\mathbf{1}^{-}$ and $\mathbf{1}^{2-}$ to interact strongly with transition metal cations would not only be theoretically interesting[19b,c] but would also expand the list of their potential applications beyond the strict field of molecular magnetism. For instance, with their tunability and analogous relationships to semiquinones and catecholate dianions, this new class of compounds offers potential opportunities to give cooperative behavior related to valence tautomerism.[20] Similarly, they may also give access to novel organic charge-transfer materials reminiscent of those made from tetracyanobenzoquinone dimethide (TCNQ) or tetracyanoethylene (TCNE) and π-electron donors.

Design of a compact structure with well-defined coordination abilities, good self-assembly prospects, potential tunability of the S−T gap, and lack of tendency toward Jahn−Teller distortions is a nontrivial challenge. Despite the caveats mentioned above, our calculations indicate that derivatives of $\mathbf{1}^{2-}$ and their metal complexes address most of the critical design issues, making them worthwhile synthetic targets. We have already synthesized and characterized four aryl-substituted derivatives of tetrone **1** and the anions obtained by their reductions are currently being structurally, spectroscopically, and electrochemically investigated. The rather encouraging results from these efforts will be reported in due course.

Computational Details

All calculations with the 6-31G*[21] basis set were performed with the GAMESS D98[22] program running on a SGI/CRAY Origin 2000 computer. Geometries of all complexes in both electronic states were fully optimized in D_{2h} symmetry at each level of calculation. The lowest energy orbitals with the symmetries listed in Figure 3 were selected as the active space. Due to the very low electron occupation of the LUMO+1 in the triplet CAS(2,3), calculations were automatically terminated by the program. Since GAMESS D98 cannot calculate analytical derivatives at the MCSCF level, vibrational frequencies were calculated only at the CAS(2,2) level with the use of the GVB method for singlet and ROHF for triplet (these methods gave the same single point energies as CAS(2,2)). The symmetry-adapted CAS(14,12) active space generates 70 840 configurations for the triplet state and 42 756 for the singlet state. Multiconfigurational GAMESS calculations that were attempted with the 6-31+G* basis set failed to converge. They were, however, successfully completed by use of the Molpro package[23,24] after verification that this software yielded identical results to GAMESS D98 for the 6-31G* basis set.

Acknowledgment. This work was partially supported by the National Computational Science Alliance (NCSA) under CHE990017N (we utilized the NCSA SGI/CRAY Origin 2000) and by NSF funds [DMR-9610335] to J.E.J. and James L. Dye. We also gratefully acknowledge useful discussions with Professor Piotr Piecuch and his research group.

Note Added after ASAP: The captions to Figures 3 and 4 were reversed and there was a misspelling in an author's name in the version posted ASAP April 27, 2001; the corrected version was posted May 1, 2001.

Supporting Information Available: Coordinates of the unique atoms of all optimized geometries of complexes of $\mathbf{1}^{2-}$ and their vibrational frequencies calculated at TCSCF and ROHF/6-31G* levels (PDF). This material is available free of charge via the Internet at http://pubs.acs.org.

JA0021417

---

(19) (a) Pontillon, Y.; Bencini, A.; Caneschi, A.; Dei, A.; Gatteschi, D.; Gillon, B.; Sangregorio, C.; Stride, J.; Totti, F. *Angew. Chem., Int. Ed. Engl.* **2000**, *39*, 1786. (b) Rodriguez, J. H.; Wheeler, D. E.; McCusker, J. K. *J. Am. Chem. Soc.* **1998**, *120*, 12051. (c) Wheeler, D. E.; Rodriguez, J. H.; McCusker, J. K. *J. Phys. Chem. A* **1999**, *103*, 4101.

(20) (a) Gutlich, P.; Dei, A. *Angew. Chem., Int. Ed. Engl.* **1997**, *36*, 2734. (b) Pierpont, C. G.; Lange, C. W. *Prog. Inorg. Chem.* **1994**, *41*, 331. (c) Pierpont, C. G.; Buchanan, R. M. *Coord. Chem. Rev.* **1981**, *38*, 45.

(21) Hariharan, P. C.; Pople, J. A. *Theor. Chim. Acta* **1973**, *28*, 213.

(22) Schmidt, M. W.; Baldridge, K. K.; Boatz, J. A.; Elbert, S. T.; Gordon, M. S.; Jensen, J. H.; Koseki, S.; Matsunaga, N.; Nguyen, K. A.; Su, S. J.; Windus, T. L.; Dupuis, M.; Montgomery, J. A. *J. Comput. Chem.* **1993**, *14*, 1347.

(23) Werner, H. J.; Knowles, P. J. *J. Chem. Phys.* **1985**, *82*, 5053.

(24) Knowles, P. J.; Werner, H. J. *Chem. Phys. Lett.* **1985**, *115*, 259.